Journal of Marine Systems 167 (2017) 33–42

Contents lists available at ScienceDirect

Journal of Marine Systems

journal homepage: www.elsevier.com/locate/jmarsys

# Biogeochemical properties of sinking particles in the southwestern part of the East Sea (Japan Sea)

Minkyoung Kim [a], Jeomshik Hwang [a,*], TaeKeun Rho [b], Tongsup Lee [c], Dong-Jin Kang [b], Kyung-Il Chang [a], Suyun Noh [a], HuiTae Joo [c], Jung Hyun Kwak [d], Chang-Keun Kang [d], Kyung-Ryul Kim [e]

[a] School of Earth and Environmental Sciences/Research Institute of Oceanography, Seoul National University, Seoul, South Korea
[b] Korea Institute of Ocean Science & Technology, Ansan, South Korea
[c] Department of Oceanography, Pusan National University, Busan, South Korea
[d] School of Environmental Science and Engineering, Gwangju Institute of Science & Technology, Gwangju, South Korea
[e] GIST College, Gwangju Institute of Science and Technology, Gwangju, South Korea

ARTICLE INFO

*Article history:*
Received 22 February 2016
Received in revised form 22 July 2016
Accepted 4 November 2016
Available online 9 November 2016

*Keywords:*
Particulate organic carbon
Biological pump
Sediment trap
Radiocarbon
Sediment resuspension
East Sea (Japan Sea)

ABSTRACT

This study investigates the biological pump system in the East Sea (Japan Sea) by conducting an analysis of the total particle flux, biogenic material composition, and carbon isotope ratios of sinking particles. The samples were collected for one year starting from March 2011 using time-series sediment traps deployed at depths of 1040 m and 2280 m on bottom-tethered mooring at Station EC1 (37.33°N, 131.45°E; 2300 m water depth) in the Ulleung Basin (UB), southwestern part of the East Sea. The temporal variation in the particulate organic carbon (POC) flux at 1000 m shows a good relationship with the primary production in the corresponding surface water. The ratio of POC flux at 1000 m to satellite-based primary production in the corresponding region in the UB was ~3%, which is comparable to the values of 2 to 5% estimated from previous studies of other part of the East Sea. The lithogenic material accounted for >17% of the sinking particles at 1000 m and for a larger fraction of 40 to 60% at 2280 m. The radiocarbon contents of the sinking POC at both trap depths imply the additional supply of aged POC, with a much greater contribution at 2280 m. Overall, the particle flux in the deep interior of the East Sea appears to be controlled by the supply of complex sources, including aeolian input, the lateral supply of resuspended sediments, and biological production in the surface water.



## 1. Introduction

The East Sea (also known as the Japan Sea) is a marginal sea surrounded by the Asian continent, the Korean peninsula, and the Japanese islands. The East Sea is connected to the Pacific Ocean through shallow straits (Fig. 1), and the surface water in the East Sea, especially south of the subpolar front at ~40°N, is mainly supplied by the Tsushima Warm Current flowing through the Korea Strait (Cho and Kim, 2000).

A study of primary production based on satellite observations showed that the southwestern part, the Ulleung Basin (UB), was the most productive region in the East Sea (Yamada et al., 2005). For the UB, the annual primary production determined using monthly *in situ* measurements (273 gC $m^{-2}$ $yr^{-1}$; Kwak et al., 2013a) and Moderate Resolution Imaging Spectroradiometer (MODIS-aqua) satellite observations (280 gC $m^{-2}$ $yr^{-1}$; Joo et al., 2014) is reportedly higher than that of the Kuroshio region (where the Tsushima Warm Current bifurcates), the East China Sea, and the Northwestern Pacific Ocean at similar latitudes (Kwak et al., 2013a, 2013b).

A few hypotheses have been suggested to explain the high annual primary productivity in this region. Frequent upwelling in the southeast coast of Korea was observed to supply nutrients supporting a local enhancement in primary production, and nutrients and particulate organic matter may be further transported into the basin via the surface current (Yoo and Park, 2009). Another hypothesis points out the importance of the vertical structure of the water column in the UB. Especially in summer when the surface mixed layer is much shallower than the euphotic depth, upward flux of nitrate from the underlying nutrient-abundant water supports the primary production (Kwak et al., 2013b). The high production in summer in the subsurface chlorophyll maximum was suggested as another main cause of the high annual primary productivity in this region (Rho et al., 2012). Another study suggested that the quantity of nutrients supplied by the current flowing into the UB through the Korea Strait is enough to sustain the observed primary productivity (Lee and Rho, 2013).

The organic carbon content in the surface sediment of the UB is >2% (Cha et al., 2007; Lee et al., 2008), which is unusually high considering its bottom depth of 2300 m. This value is comparable to those observed

* Corresponding author at: School of Earth and Environmental Sciences, Seoul National University, Seoul 08826, South Korea.
*E-mail address:* jeomshik@snu.ac.kr (J. Hwang).

http://dx.doi.org/10.1016/j.jmarsys.2016.11.001
0924-7963/

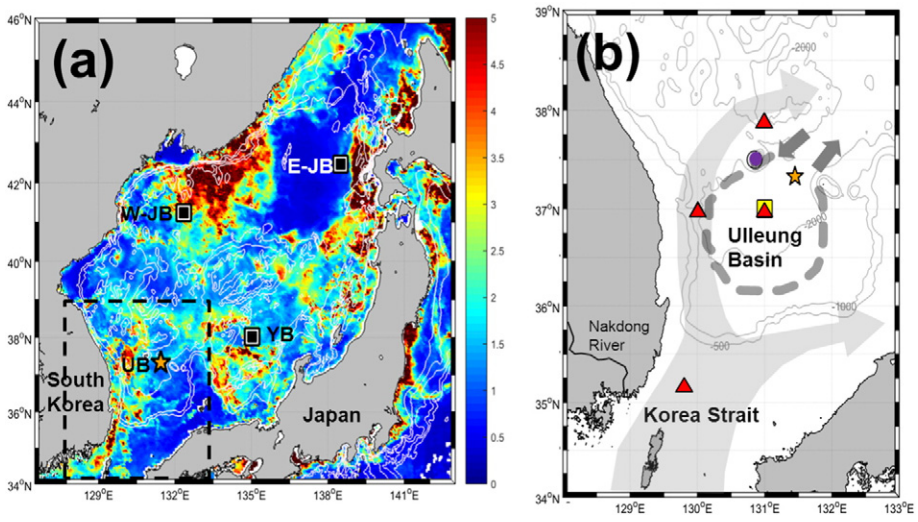


**Fig. 1.** (a) A map of the study site with the average chlorophyll-a concentration in April 2011 derived from MODIS satellite data with 4 km spatial resolution (http://oceandata.sci.gsfc.nasa.gov/). Locations of sediment trap mooring sites in this study (star) and in other basins (square; Otosaka et al., 2008) are indicated. (b) Blow-up map of the Ulleung Basin. Sampling sites for sinking particles (star), suspended particles (triangle), and core-top sediment (0–1 cm; open square) are indicated. The location of Ulleungdo island (circle) in which aerosol concentration and precipitation data were collected is also indicated. A schematic of deep currents (shaded dashed arrow; Chang et al., 2009) and major surface currents (shaded solid arrows; Kwak et al., 2013b) is also shown.

in highly productive regions such as the Chilean upwelling region (Schubert et al., 2000; Böning et al., 2005). The riverine input of organic matter from the Korean peninsula and the Japanese islands is much smaller when compared to the *in situ* primary production (Hong et al., 1997). Therefore, the high organic carbon content in the basin sediment implies a high supply of marine organic carbon into the basin sediment. The potential for a high export flux of particulate organic carbon (POC) was implied by the relatively high *f*-ratio values (~0.6) estimated using the nitrate and ammonium uptake rates in the UB (Kwak et al., 2013b). Nevertheless, the sinking particle flux to the basin interior and the biological carbon pump operation in this region are not well understood.

In this paper, we present the one year fluxes and biogeochemical compositions of sinking particles collected at 1040 m and 2280 m on bottom-tethered mooring in the UB. We examined the biogeochemical properties, including the radiocarbon content and excess Mn, in sinking particle samples to better understand the particle supply to the basin. Then, we compare our results for the UB with previously reported data from other major basins in the East Sea to obtain a more comprehensive picture of the particle transport dynamics.

## 2. Methods

### 2.1. Sample collection

Sinking particles were collected for one year from March 2011 by using time-series sediment traps with a conical type with an aperture diameter of 80 cm and height/diameter ratio of 1.32 (SMD-26S-6000, Nichiyu Giken Kogyo Co., Ltd., Japan) deployed at 1040 m (nominal depth of 1000 m hereafter) and 2280 m (20 m above the seafloor, nominal depth of 2300 m hereafter) on bottom tethered mooring at Station EC1 (37.33°N, 131.45°E; 2300 m water depth; Fig. 1) in the UB. This station has been occupied since 1996 mainly for physical oceanographic studies (Chang et al., 2002). The mooring also carried a 75 kHz ADCP at 465 m, RCM-type current meters at 1000 m, 1400 m, and 2200 m together. The subsurface currents were measured every 30 min. Sampling interval for each cup of the sediment traps was programmed to be between 10 and 17 days (Table 1) based on the expected seasonal primary productivity in the UB. The sampling cups of the traps were filled with artificial seawater containing 35 g NaCl per liter and saturated $HgCl_2$ solution as a preservative (5% final concentration). Recovered samples were stored at 4 °C in a refrigerator until further treatment.

In August 2011, the suspended particles were collected aboard the survey vessel *Haeyang 2000* by using a plankton net (30 cm diameter, 20 μm mesh size) at the surface layer (0 to 2 m) at 4 locations (37.00°N, 131.00°E; 37.00°N, 130.00°E; 37.87°N, 131.00°E; and 35.18°N, 129.80°E; Fig. 1). The particles were filtered on a GF/F filter (Whatman, 0.7 μm nominal pore size, pre-baked at 450 °C for 4 h) on board and were stored frozen at −20 °C. A sediment sample was collected using a box core (canister size = 30 × 30 × 30 cm) at the center of the UB (37.00°N, 131.00°E; Fig. 1). The sediment in the canister was sub-sampled with 5 cm diameter plastic barrels. The sediment core was sliced into 1–2 cm layers on board and then the sediment samples were stored frozen at −20 °C in pre-baked glass jars.

### 2.2. Sample analyses

In the laboratory, each sinking particle sample was filtered with a 1 mm nylon mesh to remove swimmers and any large particles, and was then divided into 10 equal aliquots using a wet sample divider (McLane Research Laboratories, WSD-10). An aliquot of each sample was filtered on a Nuclepore filter by first rinsing with supernatant and ultrapure water, and dried at ~45 °C in an oven. The dried samples were weighed to take gravimetric measurements of the total particle flux. After weighing, the samples were scraped off the filters and homogenized by grinding with the back tip of a glass Pasteur pipet. The amount of particles collected in bottles #21 to #26 of the 2300 m trap was extremely small so only the total mass flux was determined for these samples.

To conduct the organic carbon (OC) content and carbon isotope analyses, ~20 mg of each homogenized particle sample were weighed in a silver cup and fumigated with concentrated HCl in a desiccator for ~20 h at room temperature to remove inorganic carbon (Hedges and Stern, 1984; Komada et al., 2008). After fuming, each sample was placed on a hot plate at ~45 °C for 4 h to remove the remaining HCl vapor and then transferred into a quartz tube with CuO. The quartz tube was evacuated on a vacuum line, flame-sealed, and then combusted at 850 °C for 4 h. The resulting gas was cryogenically purified and the $CO_2$ gas was stored in a Pyrex tube. The organic carbon content of each sample was determined by the manometrically determined amount of $CO_2$ obtained from the closed tube combustion. The relative standard deviation (RSD) of this method is ±3%, based on the repetitive processing of glucose. For the suspended particle samples, a fraction of the GF/F filter with

**Table 1**
Sampling time, cup open interval, fluxes of total particles and POC, concentrations of biogenic and lithogenic components, carbon isotope values, and Al and Mn concentrations of sinking particles. Values in parenthesis are the contents of POM, opal, and $CaCO_3$ estimated from the elemental values. ND denotes not-determined.

| Cup # | Cup opening date (mm/dd/yy) | Sampling interval (days) | Total Mass flux (mg $m^{-2}$ $d^{-1}$) | POC flux (mg C $m^{-2}$ $d^{-1}$) | POC (POM) % | Bio-Si (Opal) % | PIC ($CaCO_3$) % | Lithogenic particles (%) | C/N ratio | $\Delta^{14}C$ (‰) | $\delta^{13}C$ (‰) | Al (%) | Mn (ppm) |
|---|---|---|---|---|---|---|---|---|---|---|---|---|---|
| 1000 m | | | | | | | | | | | | | |
| 1 | 03/15/11–04/01/11 | 17 | 365 | 19 | 5.2 (13) | 25 (60) | 0.9 (7.8) | 23 | 8.8 | −41 | −22.4 | 1.9 | 2.8E + 2 |
| 2 | 04/01/11–04/11/11 | 10 | 652 | 37 | 5.7 (14) | 26 (62) | 0.9 (7.2) | 19 | 9.1 | −25 | −22.0 | 1.6 | 2.1E + 2 |
| 3 | 04/11/11–04/21/11 | 10 | 648 | 42 | 6.5 (16) | 27 (64) | 1.3 (10.7) | 18 | 8.6 | −15 | −23.1 | 1.5 | 1.9E + 2 |
| 4 | 04/21/11–05/01/11 | 10 | 399 | 25 | 6.2 (16) | 25 (59) | 1.7 (13.9) | 20 | 8.7 | −11 | −22.8 | 1.7 | 3.0E + 2 |
| 5 | 05/01/11–05/11/11 | 10 | 817 | 53 | 6.4 (16) | 23 (54) | 2.1 (17.7) | 17 | 9.5 | −5 | −22.5 | 1.4 | 2.4E + 2 |
| 6 | 05/11/11–05/21/11 | 10 | 322 | 22 | 7.0 (17) | 20 (49) | 2.3 (19.1) | 20 | 9.5 | −7 | −23.1 | 1.6 | 3.2E + 2 |
| 7 | 05/21/11–06/01/11 | 11 | 245 | 18 | 7.4 (19) | 15 (35) | 1.8 (15.1) | 39 | 10.1 | −31 | −24.1 | 3.2 | 5.1E + 2 |
| 8 | 06/01/11–06/16/11 | 15 | 121 | 11 | 8.8 (22) | 10 (24) | 1.7 (14.5) | 46 | 10.2 | −54 | −24.7 | 3.8 | 5.3E + 2 |
| 9 | 06/16/11–07/01/11 | 15 | 347 | 33 | 9.6 (24) | 6 (14) | 3.1 (25.7) | 26 | 9.7 | −5 | −23.5 | 2.2 | 3.9E + 2 |
| 10 | 07/01/11–07/16/11 | 15 | 281 | 27 | 9.8 (24) | 9 (21) | 3.2 (26.9) | 31 | 9.3 | 4 | −23.2 | 2.5 | 4.3E + 2 |
| 11 | 07/16/11–08/01/11 | 16 | 131 | 12 | 9.1 (23) | 11 (27) | 2.4 (19.9) | 35 | 9.7 | 4 | −23.7 | 2.9 | 3.9E + 2 |
| 12 | 08/01/11–08/16/11 | 15 | 246 | 24 | 9.6 (24) | 5 (11) | 1.2 (10.2) | 51 | 9.7 | −10 | −23.8 | 4.2 | 4.7E + 2 |
| 13 | 08/16/11–09/01/11 | 16 | 247 | 22 | 8.9 (22) | 13 (30) | 1.0 (8.5) | 36 | 9.3 | −8 | −23.6 | 2.9 | 6.4E + 2 |
| 14 | 09/01/11–09/16/11 | 15 | 318 | 25 | 7.7 (19) | 16 (38) | 1.1 (8.9) | 39 | 9.3 | −20 | −23.5 | 3.2 | 5.1E + 2 |
| 15 | 09/16/11–10/01/11 | 15 | 397 | 28 | 6.9 (17) | 17 (41) | 1.0 (8.0) | 41 | 8.7 | −16 | −23.1 | 3.4 | 6.0E + 2 |
| 16 | 10/01/11–10/11/11 | 10 | 609 | 37 | 6.0 (15) | 19 (45) | 0.9 (7.2) | 35 | 9.0 | −7 | −22.5 | 2.9 | 6.5E + 2 |
| 17 | 10/11/11–10/21/11 | 10 | 413 | 28 | 6.8 (17) | 18 (43) | 1.2 (10.2) | 27 | 9.2 | −2 | −22.8 | 2.3 | 6.8E + 2 |
| 18 | 10/21/11–11/01/11 | 11 | 285 | 21 | 7.4 (19) | 20 (47) | 1.2 (10.2) | 34 | 8.5 | −9 | −23.1 | 2.8 | 7.6E + 2 |
| 19 | 11/01/11–11/16/11 | 15 | 405 | 27 | 6.7 (17) | 16 (39) | 1.6 (13.4) | 37 | 7.5 | −3 | −22.5 | 3.0 | 8.2E + 2 |
| 20 | 11/16/11–12/01/11 | 15 | 182 | 12 | 6.7 (17) | 15 (36) | 2.0 (16.7) | 36 | 8.8 | −5 | −22.8 | 3.0 | 4.2E + 2 |
| 21 | 12/01/11–12/16/11 | 15 | 78 | 6.6 | 8.4 (21) | 13 (31) | 1.6 (13.2) | 40 | 8.6 | −8 | −23.0 | 3.3 | 3.4E + 2 |
| 22 | 12/16/11–01/01/12 | 16 | 59 | 4.1 | 6.9 (17) | 13 (32) | 3.2 (26.6) | 41 | 7.0 | −71 | −24.0 | 3.4 | 3.6E + 2 |
| 23 | 01/01/12–01/11/12 | 10 | 51 | 5.2 | 10 (25) | 14 (34) | ND | 53 | 9.5 | −16 | −23.2 | 4.3 | 8.2E + 2 |
| 24 | 01/11/12–01/21/12 | 10 | 39 | 3.5 | 8.9 (22) | | ND | | ND | −69 | −23.9 | | |
| 25 | 01/21/12–02/01/12 | 11 | 56 | 3.7 | 6.6 (16) | 11 (26) | 1.1 (9.2) | 64 | 8.7 | −50 | −22.9 | 5.2 | 8.1E + 2 |
| 26 | 02/01/12–02/16/12 | 15 | 40 | 2.8 | 7.0 (17) | | 1.3 (10.5) | | 8.3 | −44 | −23.0 | | |
| 2300 m | | | | | | | | | | | | | |
| 1 | 03/15/11–04/01/11 | 17 | 347 | 16 | 4.6 (11) | 16 (38) | 0.6 (4.7) | 50 | 9.2 | −79 | −22.3 | 4.1 | 3.9E + 3 |
| 2 | 04/01/11–04/11/11 | 10 | 619 | 33 | 5.3 (13) | 22 (52) | 0.4 (3.4) | 40 | 9.3 | ND | ND | 3.3 | 1.2E + 3 |
| 3 | 04/11/11–04/21/11 | 10 | 683 | 38 | 5.5 (14) | 19 (45) | 0.7 (5.6) | 40 | 9.5 | −33 | −22.3 | 3.3 | 2.6E + 3 |
| 4 | 04/21/11–05/01/11 | 10 | 503 | 26 | 5.2 (13) | 17 (40) | 0.1 (0.4) | 47 | 8.8 | ND | ND | 3.8 | 4.7E + 3 |
| 5 | 05/01/11–05/11/11 | 10 | 1109 | 57 | 5.2 (13) | 17 (42) | 1.5 (12.1) | 36 | 8.4 | −32 | −22.6 | 2.9 | 4.2E + 3 |
| 6 | 05/11/11–05/21/11 | 10 | 674 | 35 | 5.2 (13) | 16 (39) | 1.6 (13.4) | 42 | 9.3 | ND | ND | 3.5 | 4.9E + 3 |
| 7 | 05/21/11–06/01/11 | 11 | 281 | 12 | 4.4 (11) | 14 (34) | 1.1 (9.3) | 56 | 9.3 | −90 | −23.3 | 4.6 | 6.1E + 3 |
| 8 | 06/01/11–06/16/11 | 15 | 216 | 11 | 4.9 (12) | 13 (30) | 1.1 (8.8) | 61 | 9.2 | −81 | −23.5 | 5.0 | 8.2E + 3 |
| 9 | 06/16/11–07/01/11 | 15 | 398 | 22 | 5.6 (14) | 10 (24) | 1.6 (13.6) | 58 | 8.9 | −52 | −23.0 | 4.8 | 8.3E + 3 |
| 10 | 07/01/11–07/16/11 | 15 | 620 | 44 | 7.1 (18) | 8 (19) | 2.2 (18.2) | 50 | 9.5 | −13 | −23.0 | 4.1 | 5.7E + 3 |
| 11 | 07/16/11–08/01/11 | 16 | 139 | 7.9 | 5.7 (14) | 9 (20) | 1.7 (14.3) | 59 | 8.5 | ND | ND | 4.8 | 4.0E + 3 |
| 12 | 08/01/11–08/16/11 | 15 | 534 | 36 | 6.7 (17) | 9 (21) | 1.0 (8.7) | 58 | 10.2 | −34 | −23.2 | 4.7 | 1.1E + 4 |
| 13 | 08/16/11–09/01/11 | 16 | 280 | 16 | 5.6 (14) | 7 (16) | 0.7 (5.9) | 59 | 9.7 | ND | ND | 4.8 | 1.2E + 4 |
| 14 | 09/01/11–09/16/11 | 15 | 447 | 26 | 5.8 (15) | 9 (22) | 0.6 (4.9) | 56 | 9.7 | −41 | −22.8 | 4.6 | 1.3E + 4 |
| 15 | 09/16/11–10/01/11 | 15 | 375 | 23 | 6.2 (15) | 12 (30) | 0.4 (3.5) | 56 | 9.1 | ND | ND | 4.6 | 1.0E + 4 |
| 16 | 10/01/11–10/11/11 | 10 | 633 | 36 | 5.8 (14) | 15 (35) | 0.4 (3.4) | 45 | 7.6 | −36 | −22.5 | 3.7 | 6.0E + 3 |
| 17 | 10/11/11–10/21/11 | 10 | 620 | 36 | 5.7 (14) | 15 (36) | 0.6 (4.6) | 45 | 9.8 | ND | ND | 3.7 | 6.9E + 3 |
| 18 | 10/21/11–11/01/11 | 11 | 411 | 24 | 5.9 (15) | 15 (37) | 0.8 (6.8) | 48 | 9.6 | −37 | −23.1 | 3.9 | 9.1E + 3 |
| 19 | 11/01/11–11/16/11 | 15 | 322 | 19 | 5.8 (15) | 12 (29) | 0.8 (6.5) | 52 | 9.5 | ND | ND | 4.3 | 1.3E + 4 |
| 20 | 11/16/11–12/01/11 | 15 | 126 | 7.8 | 6.2 (15) | 12 (30) | 0.1 (1.2) | 45 | 8.7 | −44 | −23.4 | 3.7 | 1.4E + 4 |
| 21 | 12/01/11–12/16/11 | 15 | 3.2 | ND | ND | ND | ND | ND | ND | ND | ND | ND | ND |
| 22 | 12/16/11–01/01/12 | 16 | 1.4 | ND | ND | ND | ND | ND | ND | ND | ND | ND | ND |
| 23 | 01/01/12–01/11/12 | 10 | 0.4 | ND | ND | ND | ND | ND | ND | ND | ND | ND | ND |
| 24 | 01/11/12–01/21/12 | 10 | 0.6 | ND | ND | ND | ND | ND | ND | ND | ND | ND | ND |
| 25 | 01/21/12–02/01/12 | 11 | 0.3 | ND | ND | ND | ND | ND | ND | ND | ND | ND | ND |
| 26 | 02/01/12–02/16/12 | 15 | 0.1 | ND | ND | ND | ND | ND | ND | ND | ND | ND | ND |

particles was subsampled and processed following the same method, except that silver wire was added instead of a silver cup. The $CO_2$ samples were analyzed for radiocarbon and stable carbon isotopes at the National Ocean Sciences Accelerator Mass Spectrometry Facility at the Woods Hole Oceanographic Institution (NOSAMS WHOI) by following standard techniques (McNichol et al., 1994). The uncertainty for such samples was determined by multiple duplicate-analyses in our lab to be smaller than 10‰ for $\Delta^{14}C$ [a fractionation-corrected value of $^{14}C/^{12}C$ relative to oxalic acid standard, Broecker and Olson (1959); Stuiver and Polach (1977)] and 0.1‰ for $\delta^{13}C$.

The total carbon (TC) and total nitrogen (TN) contents were analyzed using an elemental analyzer (Flash EA 1112series, CE Instruments) at the Korea Basic Science Institute, with an uncertainty of 0.9 and 1.7% RSD, respectively, based on duplicate analyses of 5 samples. The particulate inorganic carbon (PIC) content was estimated by taking the difference between the TC and OC contents. The concentrations of Si, Al, Ca, and Mn were analyzed using an ICP-AES (Optima 8300, PerkinElmer) at the Korea Basic Science Institute, with an RSD of 0.7–2.8% based on duplicate analyses of 3 samples. Each pair of cups (#23 and #24, and #25 and #26) from the 1000 m trap was combined in this analysis because of small sample amounts.

The $CaCO_3$ content was estimated by multiplying the PIC content by 8.33. Opal content was estimated by multiplying the content of biogenic Si by 2.4 with the latter estimated by subtracting lithogenic Si (3.5 × Al) from the total Si (%) (DeMaster, 1981; Mortlock and Froelich, 1989). The particulate organic matter (POM) content was estimated by multiplying

the POC content by 2.5 (Thunell, 1998). Lithogenic material content was estimated by multiplying the Al content (%) by 12.15 (Taylor and McLennan, 1985).

## 3. Results

### 3.1. Particle flux

The total particle flux (<1 mm) ranged between 39 and 817 mg $m^{-2}$ $d^{-1}$ at 1000 m (Fig. 2a). At 1000 m, the particle flux showed a peak in early May with a dip in late April immediately before the peak. Another peak was observed in the particle flux in the fall. The particle flux decreased gradually from early November to low values of ~50 mg $m^{-2}$ $d^{-1}$. In general, the total particle flux at 2300 m exhibited a similar temporal variation to that at 1000 m. However, the flux at 2300 m was noticeably higher in early May, early July and early August than that at 1000 m. The annual average particle flux was 282 (349 when the values in December through February are excluded; see discussion) and 338 mg $m^{-2}$ $d^{-1}$ at 1000 m and 2300 m, respectively.

The temporal variation in the POC flux (Fig. 2b) was in phase with the total particle flux. At 1000 m, the POC flux varied between 3 and 53 mgC $m^{-2}$ $d^{-1}$ with an average of 20 mgC $m^{-2}$ $d^{-1}$ (25 mgC $m^{-2}$ $d^{-1}$ when winter values are excluded), and at 2300 m, it varied between 8 and 57 mgC $m^{-2}$ $d^{-1}$ with an average of 25 mgC $m^{-2}$ $d^{-1}$. The seasonal variation in the POC flux reflects the primary production cycle in the temperate oceans in general, with a prominent spring bloom and a moderate fall bloom (Fig. 2b). However, the POC flux was maintained at fair values, over 20 mg $m^{-2}$ $d^{-1}$ on average, during the summer. The seasonal variation in the POC flux at 2300 m was similar to that at 1000 m with the exception of a few sampling intervals when the flux was higher at the deeper depth in July and August.

At 1000 m, the opal flux ranged between 14 and 442 mg $m^{-2}$ $d^{-1}$, with an average of 120 mg $m^{-2}$ $d^{-1}$ (150 mg $m^{-2}$ $d^{-1}$ when winter values are excluded), and at 2300 m, it was between 28 and 464 mg $m^{-2}$ $d^{-1}$ with an average of 142 mg $m^{-2}$ $d^{-1}$ (Fig. 2c). A bimodal seasonal variation was more clearly observed in the opal flux than in the total particle flux, and the first and second peaks in the spring were comparable in magnitude. The opal flux in June, July, and August was low (~40 mg $m^{-2}$ $d^{-1}$) and started to increase in late September to form a fall bloom peak (~270 mg $m^{-2}$ $d^{-1}$). The flux in the winter was the lowest. In general, the opal flux at 2300 m was similar to, or lower than that at 1000 m with the exception of the values taken in the summer.

At 1000 m, the $CaCO_3$ flux ranged between 4.2 and 144 mg $m^{-2}$ $d^{-1}$ with an annual average of 39 mg $m^{-2}$ $d^{-1}$ (46 mg $m^{-2}$ $d^{-1}$ when winter values are excluded), and at 2300 m, it ranged between 1.5 and 135 mg $m^{-2}$ $d^{-1}$ with an annual average of 35 mg $m^{-2}$ $d^{-1}$ (Fig. 2d). The $CaCO_3$ flux was about one third of the opal flux, and the temporal

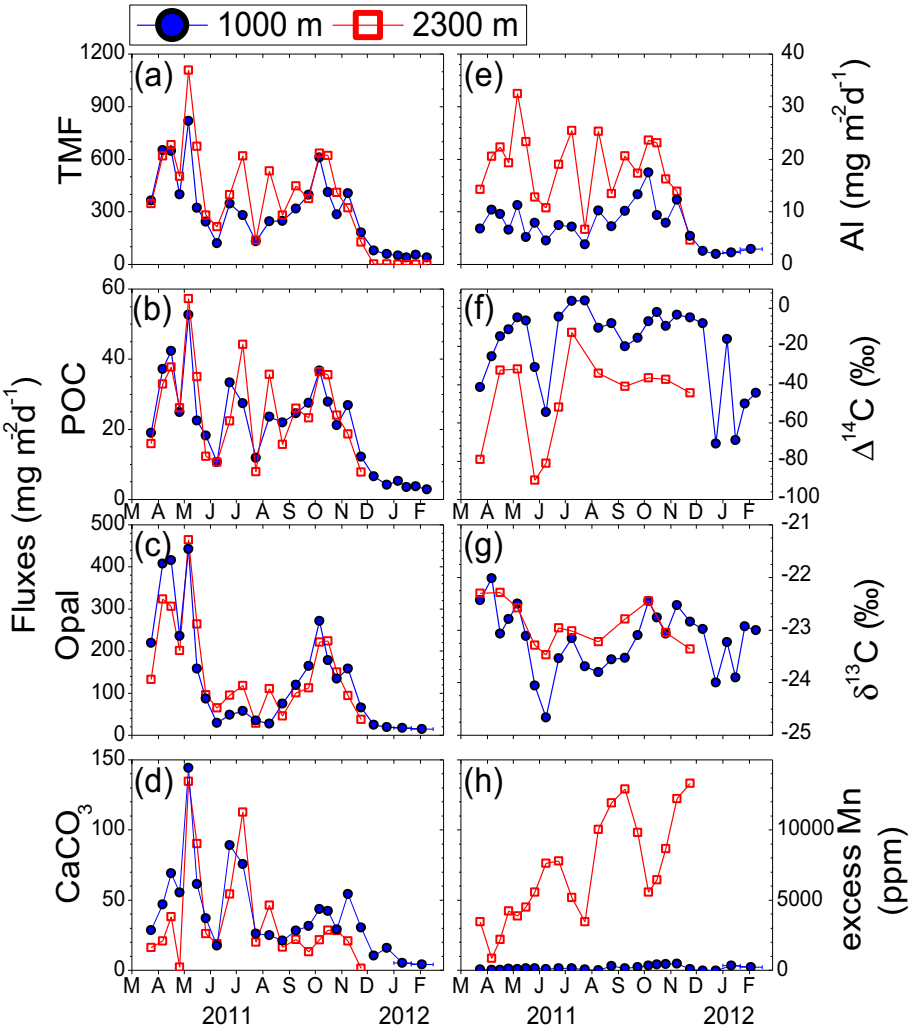


**Fig. 2.** Temporal variation in the fluxes of total particle (TMF), POC, opal, and $CaCO_3$ (left column), and Al flux, $\Delta^{14}C$ values, $\delta^{13}C$ values, and excess Mn concentration (right column) of sinking particles collected at 1000 m (circle) and 2300 m (square). The horizontal error bars denote the periods that each combined sample represents (see the text).

variation in the $CaCO_3$ was different from that of the opal flux in several aspects. The peak flux in April was about half of that in early May. Another peak amounting to 90 mg $m^{-2}$ $d^{-1}$ was observed in late June and early July. The fall bloom signal was only about one third of the spring signal. During each spring and fall bloom, the peak in $CaCO_3$ appears later than that of opal. The $CaCO_3$ flux at 2300 m was mostly lower than that at 1000 m (Fig. 2d).

The Al flux at 1000 m ranged between 2.0 and 17 mg $m^{-2}$ $d^{-1}$ with an annual average of 7.1 mg $m^{-2}$ $d^{-1}$ (8.5 mg $m^{-2}$ $d^{-1}$ when winter values are excluded) (Fig. 2e). The highest value at 1000 m was observed in early October. The temporal variation in the Al flux at 1000 m was decoupled from that of the total particle flux. The Al flux at 2300 m was larger than the flux at 1000 m and was temporally more variable, ranging between 5 and 32 mg $m^{-2}$ $d^{-1}$. The annual average Al flux at 2300 m (18 mg $m^{-2}$ $d^{-1}$) was about twice the value at 1000 m (8.5 mg $m^{-2}$ $d^{-1}$). The temporal variation in the Al flux at 2300 m was similar to that of the total particle flux.

### 3.2. Particle composition

The POC content at 1000 m varied between 5.2 and 10% with an average of 7.6% (19% as POM, Fig. 3). In general, the POC content was slightly lower in the spring and fall (~6.6%) than in the summer and winter (~8.6%). At 2300 m, the POC content varied within a narrower range between 4.4 and 7.1% (5.7% on average, 14% as POM).

The average opal content was 36% (sampling duration-weighted) at 1000 m (Fig. 3). Opal was the dominant component of the sinking particles at 1000 m in the spring and fall, and the opal content was the lowest in June and August. The $CaCO_3$ content was 14% on average at 1000 m. The temporal variation in the $CaCO_3$ content was distinct from that of opal. Higher values of the $CaCO_3$ content were observed in June, July, and late December when the opal content tended toward the lower end. The biogenic components at 2300 m varied in a similar fashion to those at 1000 m.

At 1000 m, the lithogenic material accounted for a fraction comparable to the biogenic opal (37% on average; sampling duration-weighted). In the summer and winter when the opal content was low, the lithogenic material accounted for the largest fraction of samples obtained at 1000 m. At 2300 m, the lithogenic material was the dominant component of the sinking particles (51% on average) year round with the exception of the peak spring bloom period when the opal and lithogenic components were comparable (Fig. 3).

The molar ratio of biogenic Si to PIC (Bio-Si/PIC) ranged between 2 and 30 at 1000 m and between 4 and 90 at 2300 m (not shown). The temporal variations at 1000 m and 2300 m were similar although the average value of this ratio was higher at 2300 m (22 ± 21%) than at 1000 m (12 ± 8%). The organic carbon to total nitrogen molar ratio (OC/TN) varied between 7 and 10, with average values of 9.0 ± 0.7% and 9.2 ± 0.6% at 1000 m and 2300 m, respectively (not shown; Table 1).

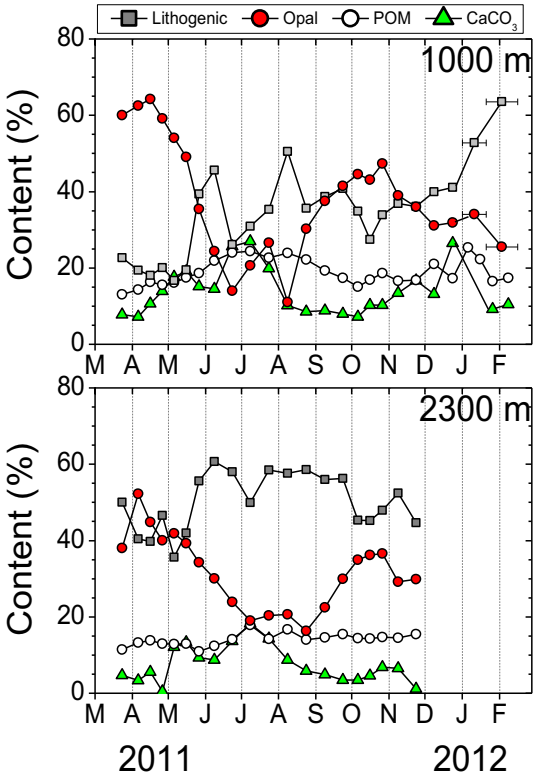


**Fig. 3.** Relative concentrations (%) of biogenic and lithogenic components in sinking particles (square = lithogenic, closed circle = opal, open circle = organic matter, triangle = $CaCO_3$) at 1000 m (top) and at 2300 m (bottom).

### 3.3. Carbon isotopic compositions

The $\Delta^{14}C$ values of sinking POC at 1000 m ranged mostly between −20‰ and +4‰, with occasional excursions to exceptionally low values (Fig. 2f). At 2300 m, most $\Delta^{14}C$ values ranged between −52‰ and −32‰. A relatively high value of −13‰ was observed in July, and low values around −80 to −90‰ were observed in March, late May, and early June. The $\Delta^{14}C$ values at 2300 m exhibited a similar temporal variation to that at 1000 m. However, the $\Delta^{14}C$ values at 2300 m were lower than the corresponding values at 1000 m by ~30‰ on average.

The $\delta^{13}C$ values of the sinking POC ranged between −24.7 and −22.0‰ with an annual average of −23.2‰ at 1000 m and between −23.5 and −22.3‰ with an annual average of −22.9‰ at 2300 m (Fig. 2g). The $\delta^{13}C$ values at 1000 m were higher during the spring and fall bloom periods than in the summer and winter. The lowest value was observed in early June when the fluxes of the biogenic particles were the lowest immediately after the spring bloom. In general, the $\delta^{13}C$ values at 2300 m followed the temporal variation at 1000 m with a smaller amplitude.

The $\Delta^{14}C$ values of the dissolved inorganic carbon (DIC) obtained between the surface and 300 m at a nearby site (37.00°N, 131.00°E) in August 2011 were +30 ± 12‰, (the uncertainty is one standard deviation of 7 samples; M. Kim and J. Hwang, unpublished data, Table 2). However, the $\Delta^{14}C$ values of the suspended POC collected from the surface water in August 2011 at 4 locations in the UB and in the Korea Strait were −43 ± 8‰ (see Fig. 1 for the sampling locations, Table 2). The average of the $\delta^{13}C$ values for suspended POC was −22 ± 1‰. The $\Delta^{14}C$ and the $\delta^{13}C$ values of the core-top sediment (0–1 cm layer) were −104‰ and −21.1‰, respectively (see Fig. 1 for sampling location, Table 2).

**Table 2**
Carbon isotope values (‰) of aeolian dust, DIC, plankton, and POC.

| | | $\Delta^{14}C$ (‰) | $\delta^{13}C$ (‰) |
|---|---|---|---|
| Aeolian deposit[a] | | | −31.7 to −28.1 |
| DIC (37.00°N, 131.00°E; 0–300 m) | | +30 ± 12 ($n$ = 7) | 0 ± 0.4 |
| Surface water suspended POC | | −43 ± 8 ($n$ = 4) | −22 ± 1 |
| Zooplankton species (0–250 m)[b] | | | −26.2 to −22.5 |
| Sinking POC | 1000 m | −71 to +4 | −24.7 to −22.0 |
| | 2200 m | −90 to −13 | −23.5 to −22.3 |
| Core-top sediment | | −104 ($n$ = 1) | −21.1 |

[a] Guo et al., 2006.
[b] Im et al., 2015.

## 4. Discussion

### 4.1. Biological carbon pump in the East Sea

The sudden dip in the total particle flux observed in late April during the spring bloom and the abnormally low values in the winter are suspicious and need to be further examined to determine whether the flux measurements were compromised because of low sediment trap efficiency possibly associated with tilting of the mooring line. The ADCP, deployed at a depth of 465 m showed three events with an abrupt increase in tilting to >10° for 2–10 days in late April, late June, and late January (Fig. 4a). These periods are accompanied by an increase in the pressure up to 50 dbar, registered with the current meters at 1000 m and 1400 m. The dip in the total mass flux in April coincided with the tilting event, but the current speed was less than ~4 cm/s at that time (Fig. 4b). It is not clear whether the flux in late June was affected by the tilting event. The decrease in particle flux in the winter started much earlier than the tilting event, lasting even after tilting had recovered in February. The particle fluxes at both trap depths were consistently low, and the possibility of a malfunction of the traps may thus be discarded. This extremely low flux in December, January, and February was not observed in an independent study that had examined the particle flux at a nearby site in the same time period (Dr. Young-Il Kim, personal communication), and hence it is likely that the trapping efficiency of our traps was compromised during this period. Therefore, we opted to exclude the results from this period when calculating the annual flux values.

The biogenic particle flux in the UB was dominated by opal, accounting for ~62% of the biogenic particle flux at 1000 m. This opal dominance is consistent with the diatom dominance and low contribution of prymnesiophytes in the phytoplankton community in this region (Kwak et al., 2013a). During bloom periods, when the contribution of lithogenic material was relatively low, the opal flux showed attenuation with depth, implying the dissolution of opal by ~28% during the vertical transport between the two depths. The $CaCO_3$ flux exceeded the opal flux only briefly in the summer. Consistently, the contribution of prymnesiophytes to the plankton community reportedly peaked from late June to early July in 2010 (Kwak et al., 2013a).

Satellite observations of the monthly primary production in the study region showed an increase from a low value in the winter in March 2011 to the spring bloom in April and May (Fig. 5; Joo et al., 2014). The primary production then decreased to a low summer value in August. The fall bloom showed a smaller magnitude and occurred in September and October, after which primary production declined to the lowest value in December. The primary production in summer was of about 620 mgC $m^{-2}$ $d^{-1}$ compared to 1100 mgC $m^{-2}$ $d^{-1}$ during the spring bloom (Fig. 5). The monthly averaged POC flux at 1000 m generally appears to reflect the primary production cycle (Fig. 5). The ratio of the POC flux at 1000 m over the primary production ranged between 2.3 and 3.9% (Fig. 5). On average, the annual POC flux corresponded to 3.4% of the annual primary production, and this value tended toward the higher end of the range observed globally (Fischer et al., 2000). The *f*-ratio values obtained from nitrate and ammonium uptake rates in the euphotic zone in May 2010 and June 2011 were slightly higher in the fall and winter, when compared to the values in the spring and summer (~0.4; Kwak et al., 2013b). This temporal variation in the *f*-ratio appears to be consistent with that of the POC flux/primary production ratio.

The sinking POC flux observed at 1000 m in the UB is compared to those obtained from the other major basins in the East Sea at approximately the same depths although at different times between August 2000 and July 2002 (Otosaka et al., 2008; Table 3). The results for the POC flux are available for the western Japan Basin (W-JB; the station name in the original paper was MS; 41.24°N, 132.35°E), the eastern Japan Basin (E-JB; original station name was JN; 42.47°N, 138.50°E), and the Yamato Basin (YB; original station name was JS; 38.02°N, 135.03°E). The average primary production (March 2003–December 2012) estimated for the 50 × 50 $km^2$ area corresponding to the sediment trap sites by the size-fractionated primary production algorithm based on MODIS ocean color data was 266, 212, 233, and 256 gC $m^{-2}$ $yr^{-1}$ at UB, W-JB, E-JB, and YB, respectively (Table 3). The annual average POC fluxes at ~1000 m (sampling duration-weighted), 25, 31, 12, and 24 mgC $m^{-2}$ $d^{-1}$, at UB, W-JB, E-JB, and YB, respectively, correspond to 3.4, 5.3, 1.9, and 3.4% of the annual primary production. The export efficiency (POC flux at 1000 m over primary production) in the UB was comparable to that at other sites in the East Sea. The overall export efficiency in the East Sea is ~3% on average at the 1000 m depth. However, the actual biological carbon pump efficiency is likely lower than this because sinking POC at the 1000 m also contains other sources in addition to primary production in the overlying water column (see the Discussion in the next section).

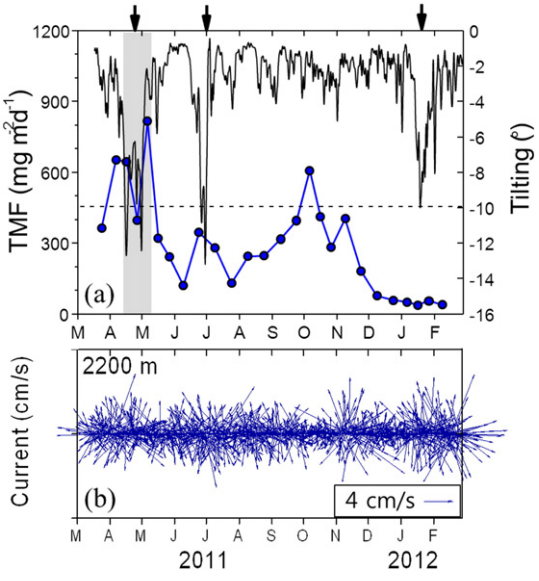


**Fig. 4.** (a) The particle flux at 1000 m and pitch tilting (solid line) determined by the ADCP deployed at the 465 m depth. The pitch tilting events amounting to 10° for 2 to10 days are indicated with arrows. (b) Current speed and direction measured every 6 h at 2200 m on the same mooring.

### 4.2. Sources of sinking particles to the mesopelagic layer

The average Al flux was 8.5 (when winter values excluded) and 18 mg $m^{-2}$ $d^{-1}$ at 1000 m and 2300 m, respectively. Consequently, the lithogenic material accounted for ~32% and ~51% of the sinking particles, respectively. The potential sources of the lithogenic material to the 1000 m trap were atmospheric input (the Asian brown dust), riverine input, lateral transport by the Tsushima Warm Current, and a lateral supply of resuspended sediment. There are no considerable rivers along the east coast of Korea. The Nakdong River, which is the largest river in the southeastern part of Korea, annually discharges 6.3 × $10^{10}$ tons of water with 4.6 × $10^6$ tons of suspended particles to the Korea Strait (Fig. 1; Park et al., 1999). About 98% of the riverine suspended particles were reportedly sedimented in the proximal and distal mud deposits along the southeastern coast of Korea (Park et al., 1999). It is possible that the remaining fraction of fluvial particles is further transported to the central UB along the surface current.

The aeolian Al deposition was estimated from dust concentration (PM10; 10 μm or smaller in diameter, hourly measurements) and precipitation at a meteorological station in nearby Ulleungdo island (data available from the Korea Meteorological Administration; www.kma.go.kr). The dry deposition was estimated as a product of the settling velocity (we used 2 cm/s with a range of 0.3 to 6.8 cm/s for the coastal or marginal seas; Hsu et al., 2009), the daily dust concentration in air, and

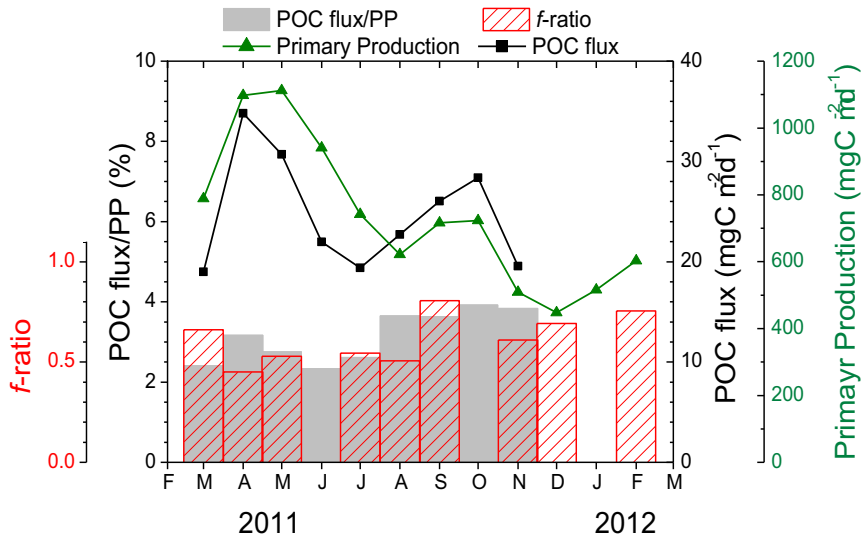


**Fig. 5.** Monthly POC flux at 1000 m, primary productivity in the surface water (Joo et al., 2014), POC flux/Primary production ratio, and *f*-ratio (Kwak et al., 2013b) in the Ulleung Basin. The major ticks on the x-axis indicate the center of each month.

the Al concentration (5.9–7.4%; Strambeanu et al., 2015). Wet deposition was estimated as a product of the daily rainfall (mm/d), scavenging ratio (we used a value of 1000, with a range between 500 and 2000; Hsu et al., 2009), volume-weighted average Al concentration (μg/m$^3$), and the inverse of the air density (~1200 g/m$^3$), as described by Duce et al. (1991). The estimated annual dry deposition of Al was ~850 mg m$^{-2}$ yr$^{-1}$ and the wet deposition was ~500 mg m$^{-2}$ yr$^{-1}$ (104 days with rain). The aeolian deposition was higher in the spring (March–mid-May), mid-October (Fig. 6a) and in January than in the rest of the year. The estimated average total (dry + wet) atmospheric deposition of Al to the UB from March 2011 to February 2012 was ~4 mg m$^{-2}$ d$^{-1}$. It should be noted that the estimated flux has a large uncertainty depending on the choice of the settling velocity and the scavenging ratio. Nevertheless, our estimate is comparable to the annual deposition flux of mineral dust (10–34 mg m$^{-2}$ d$^{-1}$ equivalent to 0.8–2.8 mg m$^{-2}$ d$^{-1}$ as in Al flux under the assumption of 8.2% Al concentration; Taylor, 1964) measured at Toyama, Tottori, and Fukuoka in Japan, in 2009 (Osada et al., 2014), and it is also comparable to the modern aeolian dust accumulation on the west coast of the Japanese islands (1.4–4.3 mg cm$^{-2}$ yr$^{-1}$ equivalent to 3.1–9.7 mg m$^{-2}$ d$^{-1}$; Uematsu et al., 1983). The estimated aeolian input of Al appears to account for a considerable fraction (~55%) of the Al flux at 1000 m (Fig. 6b). At W-JB, E-JB and YB, the annual Al flux supplied by the Asian dust at the 1000 m depth was reported to be 84, 13, and 68%, respectively (Otosaka et al., 2004).

The $\Delta^{14}$C values of the suspended POC in the surface water (−43 ± 8‰, see Fig. 1 for sampling locations) were significantly lower than the $\Delta^{14}$C values for DIC (+30 ± 12‰; Table 2). Also, the majority of $\Delta^{14}$C values for the sinking POC samples at 1000 m were higher than the values of the suspended POC (vice versa for $\delta^{13}$C values). These puzzling results imply that aged POC is supplied to the surface water in addition

**Table 3**
Primary production (gC m$^{-2}$ yr$^{-1}$) in the surface water, sinking POC flux (gC m$^{-2}$ yr$^{-1}$), $\Delta^{14}$C (‰), Al (%), Al flux (g m$^{-2}$ yr$^{-1}$), and excess Mn (ppm) of sinking particles at different depths in the water column in the major basins of the East Sea. The data of the Japan Basin and the Yamato Basin are from Otosaka et al. (2008) unless indicated otherwise.

| | | UB | W-JB | E-JB | YB |
|---|---|---|---|---|---|
| Primary production | Satellite obs. | 266 | 212 | 233 | 256 |
| | *In situ* meas. | 273[a] | | | |
| Sinking POC flux (~1000 m) | | 9.1 | 11.2 | 4.4 | 8.7 |
| $\Delta^{14}$C (‰) | | 11 ± 15 | −13 ± 18 | −21 ± 20 | −3 ± 28 |
| Al %, (Al flux) | | 2.6 (3.1) | 2.8 (4.3)[b] | 2.0 (1.0)[b] | 2.7 (2.5)[b] |
| Excess Mn (ppm) | | 0.47 × 10$^3$ | 0.95 × 10$^{3b}$ | 0.68 × 10$^{3b}$ | 1.1 × 10$^{3b}$ |
| Sinking POC flux (sampling depth, meters above bottom) | | 9.1 (2300 m, 20 mab) | 7.6 (2746 m, 678 mab) | 2.1 (3043 m, 599 mab) | 6.5 (2100 m, 800 mab) |
| $\Delta^{14}$C (‰) | | −48 ± 24 | −71 ± 29 | −103 ± 21 | −18 ± 27 |
| Al %, (Al flux) | | 4.1 (6.4) | 3.4 (3.3)[b] | 3.6 (1.2)[b] | 3.6 (3.3)[b] |
| Excess Mn (ppm) | | 7.5 × 10$^3$ | 2.6 × 10$^{3b}$ | 2.3 × 10$^{3b}$ | 2.8 × 10$^{3b}$ |

[a] Kwak et al., 2013a.
[b] Otosaka et al., 2004.

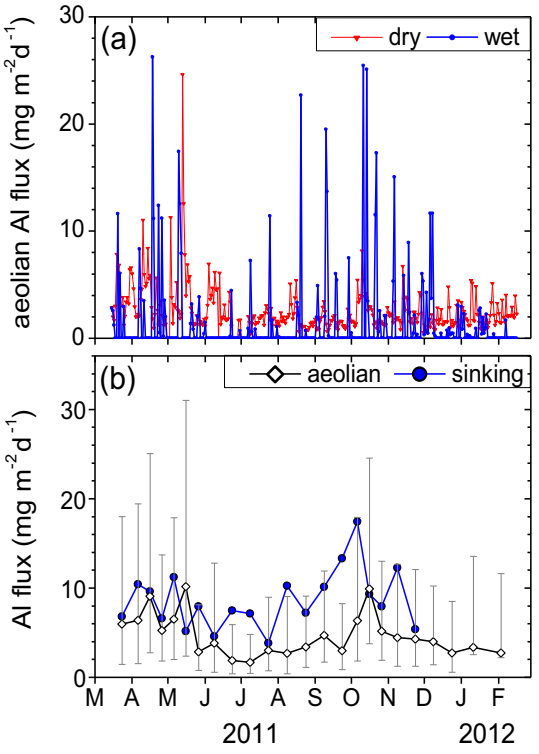


**Fig. 6.** Temporal variation of (a) atmospheric dry (reversed triangle) and wet (circle) deposition of Al estimated from aerosol concentration and precipitation data obtained in Ulleungdo island. (b) Estimated aeolian Al flux to the surface water (dry + wet deposition) and Al flux at 1000 m depth. The error bars indicate the range for the aeolian input estimate.

to *in situ* primary production. A potential source is aged POC associated with riverine suspended particles and/or aeolian lithogenic particles. Asian dust was observed to contain abundant *n*-alkanes, polycyclic aromatic hydrocarbons and fatty acids (Guo et al., 2003). The aerosols collected in northern Japan during the Asian dust season reportedly contained aged POC that probably originated from loess deposits in arid regions of China (Kawamura et al., 2010). The $\delta^{13}C$ values of the sinking POC may also support the additional supply of terrigenous organic matter. The $\delta^{13}C$ values of the suspended and sinking POC ranged between −22.0‰ and −24.7‰, and these are lower than the usually accepted value of marine POC of about −20‰ (Emerson and Hedges, 1988). Especially in June and in the winter, the $\delta^{13}C$ values of sinking POC at the 1000 m depth were considerably lower than the $\delta^{13}C$ value of the underlying sediment.

However, the POC content in aeolian dust is generally low (3% or lower; Eglinton et al., 2002), and hence, the contribution of aeolian POC to sinking POC is expected to be low (<10% based on the contribution of aeolian lithogenic particles). Sediment resuspension is another source of allochthonous, aged POC. Resuspended sediment can be laterally transported via the Tsushima Warm Current and/or deep currents inside the UB (Fig. 1). There is a wide inflow of deep water to the UB and a narrow outflow out of the UB in the western and eastern sides of the Ulleung Interplain Gap, respectively (Chang et al., 2009). Cyclonic circulation is a general feature of the deep currents inside of the UB (Fig. 1; Chang et al., 2002; Chang et al., 2009).

The contribution of aged POC to sinking POC at the 1000 m depth is hard to determine based on the $\Delta^{14}C$ mass balance because the aged POC end-member is not well defined at the study site. Furthermore, the fractionation of aged POC into the aeolian input and resuspended sediment is not feasible at this moment. As a preliminary attempt to estimate the contribution of aged POC to sinking POC, −104‰ (a value of the core-top sediment in the central basin; see Fig. 1 for the sampling location) was used for the allochthonous end-member and +30‰ for the fresh, autochthonous end-member. Based on this approach, about 30% of the sinking POC at 1000 m was estimated to have originated from allochthonous sources.

### 4.3. Dynamics of particle supply in the deep basins

Regardless of the Al flux from the overlying water column, the additional supply of Al between 1000 m and 2300 m should be derived from the lateral supply of resuspended sediment. Higher fluxes at the deeper depth occasionally observed for POC, opal, and $CaCO_3$ also indicate an additional supply of these components by sediment resuspension. At 2300 m, the $\Delta^{14}C$ values were systematically lower than those in the corresponding sampling intervals. The lowest $\Delta^{14}C$ value in late May was close to that of a core-top sediment (−104‰). Peaks occurred episodically in the Al flux at 2300 m, implying that resuspension-sedimentation likely occurred via pulse-like processes (Fig. 2e). This phenomenon may be related to the observation that near-bottom current fluctuations on timescales of 10–60 days are predominant in the Ulleung Interplain Gap (Chang et al., 2009; Kim et al., 2013).

In various locations throughout the ocean, the $\Delta^{14}C$ and Al content of sinking particles exhibit a negative correlation, implying that the main source of aged POC was sediment resuspension and that the presence of aged POC was tightly associated with resuspended clay mineral (Hwang et al., 2010). The relationship between the $\Delta^{14}C$ value and Al content (%) in the East Sea was weaker than in other locations (Fig. 7). The relationship was not statistically significant when only the 1000 m samples in the UB were considered ($p$-value = 0.42; Fig. 7). This behavior implies *i*) the input of Al with little POC or POC with $\Delta^{14}C$ values similar to that of the DIC in surface water, and/or *ii*) the occurrence of a process(es) that lower(s) the $\Delta^{14}C$ value of sinking POC without the addition of Al. The former process(es) may consist of input of aeolian dust and/or fluvial particles, as discussed earlier. The slope of the $\Delta^{14}C$- Al plot for E-JB was steeper than that of the other

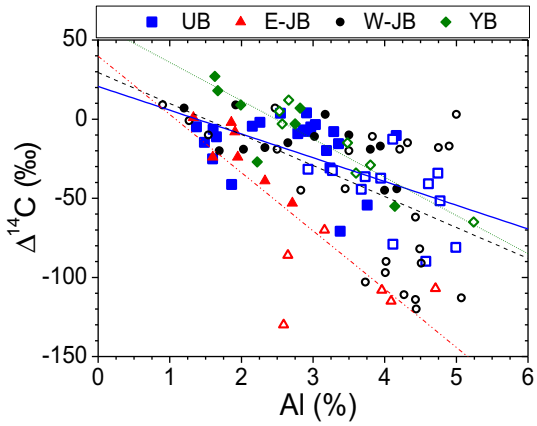


**Fig. 7.** Relationship between the $\Delta^{14}C$ values and Al content of sinking particles from the major basins of the East Sea (square = UB, triangle = E-JB, circle = W-JB, and diamond = YB). The closed symbols are the results at ~1000 m and the open symbols are the results at deeper depths.

sites (Fig. 7), and this result appears to be associated with the distinctly lower contribution of Al supplied from the Asian dust to the E-JB (13%) than that of the other sites (55–84%). The latter process(es) may include a temporal variation in the $\Delta^{14}C$ value of DIC itself in the surface water. Eddies are frequently observed in the UB, and the coastal upwelling may cause this variation (Yoo and Park, 2009). However, further examination is needed for the $\Delta^{14}C$ values of the surface water DIC to determine how these processes affect the $\Delta^{14}C$ value of DIC in the euphotic zone. Under the many caveats discussed above, the contribution of resuspended sediment ($\Delta^{14}C = -104‰$) as a representative of the allochthonous POC sources to the sinking POC at 2300 m was estimated to be about 50% based on radiocarbon mass balance.

The supply of excess Mn (Mn existing in excess of the average Mn/Al ratio of the upper crust, ~1.15%; Taylor, 1964) can be used as a proxy of the benthic source of particles near the seafloor. Soluble $Mn^{2+}$ produced via $MnO_2$ reduction in the sediment is mobilized into the water column and becomes oxidized into a particulate form by the dissolved oxygen. These particles subsequently settle to the seafloor (Yeats et al., 1979; Davison et al., 1982). The excess Mn values in the sinking particles at 1000 m in the UB were much lower than the values at 2300 m (up to $14 \times 10^3$ ppm; Fig. 2h). The excess Mn showed three broad peaks in June, September, and November, with higher values in the fall and winter in general. Reddish brown mud at the top of the sediment was visually observed upon recovery of the sediment sample from the central part of the UB. This brown layer of metalliferous sediment was only observed in the central part of the UB, and it contains a high concentration of Mn in the solid phase (~$6.6 \times 10^3$ ppm; Cha et al., 2007; Hyun et al., 2010). The excess Mn did not show any clear correlation with $\Delta^{14}C$ in the UB (this study) or in the other basins (Otosaka et al., 2008). Also, no clear correlation was observed between the excess Mn and Al flux in the UB although the correlation was strong at deep depths at W-JB ($R^2 = 0.91$) and E-JB ($R^2 = 0.89$) (calculated from the data in Otosaka et al., 2004). The excess Mn was the highest in the UB, which is at least partly caused by the vertical proximity of the sampling depth to the sea floor.

Overall, the weak correlation between $\Delta^{14}C$ of POC and the Al content in the sinking particles implies various sources of POC and lithogenic particles in the East Sea. The average $\Delta^{14}C$ values of sinking POC at depths deeper than 2000 m were −48, −71, −103, and −18‰ in the UB, W-JB, E-JB, and YB (Otosaka et al., 2008; Table 3). This basin-to-basin variation is partly caused by considerably different ages of surface sediments as sources of resuspended particles (Otosaka et al., 2008) in addition to the relative strength of sediment resuspension in each basin. The $\Delta^{14}C$ values over a wide range show the

complex behavior of POC sources and the corresponding processes for POC supply.

## 5. Summary and conclusions

Sinking particle samples at 1000 m and 2300 m (20 m above the seafloor) in the UB were collected and analyzed to investigate the biological carbon pump processes operating in the East Sea. The sinking particle flux and biogenic particle composition of the samples collected at 1000 m generally reflected the biological processes in the surface water. A considerable POC flux was observed during the summer months from June to August accounting for ~27% of the annual POC flux, which is consistent with a previous suggestion that primary production in the summer is an important contributor to the high annual production in this region (Kwak et al., 2013a; Joo et al., 2014). However, the ratio of POC flux at 1000 m over the primary production was ~3%, which is not distinct from the values obtained for other basins of the East Sea. When compared to the POC flux obtained in sediment trap studies of other basins of the East Sea, the POC flux in the UB was not significantly higher in contrast to the highest primary production obtained via satellite for the corresponding region, although the temporal variability should be considered.

The weak correlation between the $\Delta^{14}C$ values of the sinking POC and Al content of the sinking particles at 1000 m implies that the aeolian supply of both POC and lithogenic material can be an important component of the sinking particles. An estimation of the contribution by allochthonous POC to sinking POC is largely uncertain because the $\Delta^{14}C$ of allochthonous POC is not well defined. When the $\Delta^{14}C$ value of the core-top sediment in the central UB is used as the allochthonous endmember, about 30% and 50% of the sinking POC at 1000 m and 2300 m, respectively, were estimated to be derived from allochthonous sources. However, these estimates need to be refined in further studies to determine the properties of the various potential allochthonous sources.

Considering a similar or higher particle flux, low $\Delta^{14}C$ values and high excess Mn at the deeper sampling depth, the considerable lateral supply of particles in the deep interior appears to be a general feature in the East Sea. Overall, the particle flux in the deep interior of the East Sea appears to be controlled by a supply of complex POC sources with various $\Delta^{14}C$ values from aeolian input and a lateral supply of resuspended sediments, in addition to biological production in surface water. This complexity may be a characteristic of the marginal seas surrounded by continents and islands, and a careful examination of the biogeochemical and $^{14}C$-isotopic properties is needed to quantify the biological carbon pump processes and carbon preservation in the sediment of marginal seas.

## Acknowledgements

We thank the captains and the crews of the survey vessel *Haeyang 2000* and the R/V *Eardo* and cruise participants for help at sea; S.C. Hwang, Y.B. Kim, and members of the Current Dynamics Research Laboratory of Seoul National University for sediment trap deployment and recovery; staffs at NOSAMS WHOI for carbon isotopic analyses; staffs at the Korea Basic Science Institute for element and metal analyses. This research was part of the project, East Asian Seas Time series-I (EAST-I), funded by the Ministry of Oceans and Fisheries, Korea.

## References

Böning, P., Cuypers, S., Grunwald, M., Schnetger, B., Brumsack, H.J., 2005. Geochemical characteristics of Chilean upwelling sediments at ~36°S. Mar. Geol. 220, 1–21.
Broecker, W.S., Olson, E.A., 1959. Lamont radiocarbon measurements VI. Am. J. Sci. 1, 111–132.
Cha, H.J., Choi, M.S., Lee, C.B., Shin, D.H., 2007. Geochemistry of surface sediments in the southwestern East/Japan Sea. J. Asian Earth Sci. 29, 685–697.
Chang, K.I., Hogg, N.G., Suk, M.S., Byun, S.K., Kim, Y.G., Kim, K., 2002. Mean flow and variability in the southwestern East Sea. Deep-Sea Res. I 49, 2261–2279.
Chang, K.I., Kim, K., Kim, Y.B., Teague, W.J., Lee, J.C., Lee, J.H., 2009. Deep flow and transport through the Ulleung Interplain Gap in the southwestern East/Japan Sea. Deep-Sea Res. I 56, 61–72.
Cho, Y.K., Kim, K., 2000. Branching mechanism of the Tsuchima Current in the Korea Strait. J. Phys. Oceanogr. 30, 2788–2797.
Davison, W., Woof, C., Rigg, E., 1982. The dynamics of iron and manganese in a seasonally anoxic lake; direct measurement of fluxes using sediment traps. Limnol. Oceanogr. 27, 987–1003.
DeMaster, D.J., 1981. The supply and accumulation of silica in the marine environment. Geochim. Cosmochim. Acta 45, 1715–1732.
Duce, R.A., Liss, P., Merrill, J., Atlas, E., Buat-Menard, P., Hicks, B., Miller, J., Prospero, J., Arimoto, R., Church, T., 1991. The atmospheric input of trace species to the world ocean. Glob. Biogeochem. Cycles 5, 193–259.
Eglinton, T.I., Eglinton, G., Dupont, L., Sholkovitz, E.R., Montluçon, D., Reddy, C.M., 2002. Composition, age, and provenance of organic matter in NW African dust over the Atlantic Ocean. Geochem. Geophys. Geosyst. 3, 1–27.
Emerson, S., Hedges, J.I., 1988. Processes controlling the organic carbon content of open ocean sediments. Paleoceanography 3, 621–634.
Fischer, G., Ratmeyer, V., Wefer, G., 2000. Organic carbon fluxes in the Atlantic and Southern Ocean: relationship to primary production compiled from satellite radiometer data. Deep-Sea Res. II 47, 1961–1997.
Guo, Z., Sheng, L., Feng, J., Fang, M., 2003. Seasonal variation of solvent extractable organic compounds in the aerosols in Qingdao, China. Atmos. Environ. 37, 1825–1834.
Guo, Z., Li, J., Feng, J., Fang, M., Yang, Z., 2006. Compound-specific carbon isotope compositions of individual long-chain n-alkanes in severe Asian dust episodes in the North China coast in 2002. Chin. Sci. Bull. 51, 2133–2140.
Hedges, J.I., Stern, J.H., 1984. Carbon and nitrogen determinations of carbonate-containing solids. Limnol. Oceanogr. 29, 657–663.
Hong, G.H., Kim, S.H., Chung, C.S., Kang, D.J., Shin, D.H., Lee, H.J., Han, S.J., 1997. $^{210}Pb$-derived sediment accumulation rates in the southwestern East Sea (Sea of Japan). Geo-Mar. Lett. 17, 126–132.
Hsu, S.C., Liu, S.C., Arimoto, R., Liu, T.H., Huang, Y.T., Tsai, F., Lin, F.J., Kao, S.J., 2009. Dust deposition to the East China Sea and its biogeochemical implications. J. Geophys. Res. 114, D15304.
Hwang, J., Druffel, E.R., Eglinton, T.I., 2010. Widespread influence of resuspended sediments on oceanic particulate organic carbon: insights from radiocarbon and aluminum contents in sinking particles. Glob. Biogeochem. Cycles 24, GB4016.
Hyun, J.H., Mok, J.S., You, O.R., Kim, D., Choi, D.L., 2010. Variations and controls of sulfate reduction in the continental slope and rise of the Ulleung Basin off the Southeast Korean upwelling system in the East Sea. Geomicrobiol J. 27, 212–222.
Im, D.H., Wi, J.H., Suh, H.L., 2015. Evidence for ontogenetic feeding strategies in four calanoid copepods in the Eas Sea (Japan Sea) in summer, revealed by stable isotope analysis. Ocean Sci. J. 50, 481–490.
Joo, H.T., Park, J.W., Son, S.H., Noh, J.H., Jeong, J.Y., Kwak, J.H., Saux-Picart, S., Choi, J.H., Kang, C.K., Lee, S.H., 2014. Long-term annual primary production in the Ulleung Basin as a biological hot spot in the East/Japan Sea. J. Geophys. Res. 119, 3002–3011.
Kawamura, K., Matsumoto, K., Uchida, M., Shibata, Y., 2010. Contributions of modern and dead organic carbon to individual fatty acid homologues in spring aerosols collected from northern Japan. J. Geophys. Res. 115, D22310.
Kim, Y.B., Chang, K.I., Park, J.H., Park, J.J., 2013. Variability of the Dokdo Abyssal current observed in the Ulleung Interplain Gap of the East/Japan Sea. Acta Oceanol. Sin. 32, 12–23.
Komada, T., Anderson, M.R., Dorfmeier, C.L., 2008. Carbonate removal from coastal sediments for the determination of organic carbon and its isotopic signatures, $\delta^{13}C$ and $\Delta^{14}C$: comparison of fumigation and direct acidification by hydrochloric acid. Limnol. Oceanogr. Methods 6, 254–262.
Kwak, J.H., Lee, S.H., Park, H.J., Choy, E.J., Jeong, H.D., Kim, K.R., Kang, C.K., 2013a. Monthly measured primary and new productivities in the Ulleung Basin as a biological "hot spot" in the East/Japan Sea. Biogeosciences 10, 4405–4417.
Kwak, J.H., Hwang, J., Choy, E.J., Park, H.J., Kang, D.J., Lee, T., Chang, K.I., Kim, K.R., Kang, C.K., 2013b. High primary productivity and *f*-ratio in summer in the Ulleung basin of the East/Japan Sea. Deep-Sea Res. I 79, 74–85.
Lee, T., Rho, T.K., 2013. Contribution of nutrient flux through the Korea Strait to a primary production in the warm region of the East Sea. Sea 18, 65–69 (in Korean with English abstract).
Lee, T., Hyun, J.H., Mok, J.S., Kim, D., 2008. Organic carbon accumulation and sulfate reduction rates in slope and basin sediments of the Ulleung Basin, East/Japan Sea. Geo-Mar. Lett. 28, 153–159.
McNichol, A., Osborne, E., Gagnon, A., Fry, B., Jones, G., 1994. TIC, TOC, DIC, DOC, PIC, POC—unique aspects in the preparation of oceanographic samples for $^{14}C$-AMS. Nucl. Instrum. Methods Phys. Res., Sect. B 92, 162–165.
Mortlock, R.A., Froelich, P.N., 1989. A simple method for the rapid determination of biogenic opal in pelagic marine sediments. Deep-Sea Res. I 36, 1415–1426.
Osada, K., Ura, S., Kagawa, M., Mikami, M., Tanaka, T.Y., Matoba, S., Aoki, K., Shinoda, M., Kurosaki, Y., Hayashi, M., Shimizu, A., Uematsu, M., 2014. Wet and dry deposition of mineral dust particles in Japan: factors related to temporal variation and spatial distribution. Atmos. Chem. Phys. 14, 1107–1121.
Otosaka, S., Togawa, O., Baba, M., Karasev, E., Volkov, Y.N., Omata, N., Noriki, S., 2004. Lithogenic flux in the Japan Sea measured with sediment traps. Mar. Chem. 91, 143–163.
Otosaka, S., Tanaka, T., Togawa, O., Amano, H., Karasev, E.V., Minakawa, M., Noriki, S., 2008. Deep sea circulation of particulate organic carbon in the Japan Sea. J. Oceanogr. 64, 911–923.

Park, S.C., Yoo, D.G., Lee, K.W., Lee, H.H., 1999. Accumulation of recent mud associated with coastal circulations, southeastern Korea Sea (Korea Strait). Cont. Shelf Res. 19, 589–608.
Rho, T.K., Lee, T., Kim, G., Chang, K., Na, T., Kim, K.R., 2012. Prevailing subsurface chlorophyll maximum (SCM) layer in the East Sea and its relation to the physic-chemical properties of water mass. Ocean Polar Res. 34, 413–430.
Schubert, C.J., Ferdelman, T.G., Strotmann, B., 2000. Organic matter composition and sulfate reduction rates in sediments off Chile. Org. Geochem. 31, 351–361.
Strambeanu, N., Demetrovici, L., Dragos, D., 2015. Natural sources of nanoparticles. In: Lungu, M., et al. (Eds.), Nanoparticles' Promises and Risks. Springer International Publishing, pp. 9–19.
Stuiver, M., Polach, H.A., 1977. Discussion; reporting of $^{14}C$ data. Radiocarbon 19, 355–363.
Taylor, S.R., 1964. Abundance of chemical elements in the continental crust: a new table. Geochim. Cosmochim. Acta 28, 1273–1285.
Taylor, S.R., McLennan, S.M., 1985. The Continental Crust: Its Composition and Evolution. Blackwell Sci, Oxford, U.K.
Thunell, R.C., 1998. Seasonal and annual variability in particle fluxes in the Gulf of California: a response to climate forcing. Deep-Sea Res. I 45, 2059–2083.
Uematsu, M., Duce, R.A., Prospero, J.M., Chen, L., Merrill, J.T., McDonald, R.L., 1983. Transport of mineral aerosol from Asia over the North Pacific Ocean. J. Geophys. Res. 88, 5343–5352.
Yamada, K., Ishizaka, J., Nagata, H., 2005. Spatial and temporal variability of satellite primary production in the Japan Sea from 1998 to 2002. J. Oceanogr. 61, 857–869.
Yeats, P., Sundby, B., Bewers, J., 1979. Manganese recycling in coastal waters. Mar. Chem. 8, 43–55.
Yoo, S., Park, J., 2009. Why is the southwest the most productive region of the East Sea/Sea of Japan? J. Mar. Syst. 78, 301–315.